# Battery Lifetime-Aware Automotive Climate Control for Electric Vehicles

Korosh Vatanparvar, Mohammad Abdullah Al Faruque
Department of Electrical Engineering and Computer Science
University of California, Irvine, Irvine, California, USA
{kvatanpa, alfaruqu}@uci.edu

***Abstract*—Electric Vehicle (EV) optimization involves stringent constraints on driving range and battery lifetime. Sophisticated embedded systems and huge number of computing resources have enabled researchers to implement advanced Battery Management Systems (BMS) for optimizing the driving range and battery lifetime. However, the Heating, Ventilation, and Air Conditioning (HVAC) control and BMS have not been considered together in this optimization. This paper presents a novel automotive climate control methodology that manages the HVAC power consumption to improve the battery lifetime and driving range. Our experiments demonstrate that the HVAC consumption is considerable and flexible in an EV which significantly influences the driving range and battery lifetime. Hence, this influence on the above-mentioned constraints has been modeled and analyzed precisely, then it has been considered thoroughly in the EV optimization process. Our methodology provides significant improvement in battery lifetime (on average 14%) and average power consumption (on average 39% reduction) compared to the state-of-the-art methodologies.**

## I. Introduction and Related Work

Electric Vehicles (EVs) have been accepted as sustainable solution and a new paradigm of transportation [1] to address the environmental issues caused by greenhouse gases and other pollutants coming from road transportation [2]. Despite the incentives provided by governments to promote EV deployment [3], EVs pose new challenges in the trade-off between costs and performance [4]. The driving range and battery lifetime are the challenges that have become major design objectives for EVs. The cost, volume, and weight constraints in battery pack design make them the major bottleneck restricting the amount of energy stored for driving [5]. On the other hand, the battery lifetime is directly related to the State-of-Health (SoH) which represents the battery capability to store and deliver energy. The SoH degrades over time according to the battery usage pattern and the battery will become useless when it degrades for about 20% [6].

In order to alleviate the driving range and battery lifetime issue, a Battery Management System (BMS) is typically implemented to monitor and control the battery cells [1]. The BMS prevents overcharging, overdischarging, overheating, and imbalance of battery cells to improve their energy efficiency and lifetime. By presenting Hybrid Energy Storage System (HESS) [3] that may consist of ultracapacitors accompanied with battery cells, the BMS evolved to handle the charge management for heterogeneous energy storage to improve energy efficiency and battery lifetime. Other components inside EV, e.g. power converters, inverters, electrical motor, etc. demonstrate different efficiency in various conditions. Hence, the BMS may optimize the battery or HESS usage based on the components' efficiency map. Also, [3][7] have illustrated that the BMS may predict and optimize the energy consumption more efficiently by having the route information.

In the process of optimizing the energy efficiency and battery lifetime by the BMS, the electrical motor power consumption has been considered in a fine-grained level. While, up until now, the power consumption of the Heating, Ventilation, and Air Conditioning (HVAC) has been assumed to be constant. On the other hand, controlling the HVAC (automotive climate control) is mostly done using switching On/Off the system or fuzzy-based methodologies implemented on Proportional-Integral-Derivative (PID) controllers [8][9][10]. These methodologies typically try to stabilize the temperature and humidity inside the cabin within the comfort zone [11] without considering the battery lifetime. Therefore, the HVAC and the BMS have not been considered together in the optimization process. Recently, research has been done to analyze the HVAC power consumption influence on the driving range [12]. The HVAC in an EV may consume upto 6KW and reduce the driving range upto 50% depending on the outside weather conditions [13]. Hence, the HVAC power consumption is a significant factor affecting the driving range and battery lifetime, and may be controlled more easily as opposed to the electrical motor.

In summary, the above-mentioned state-of-the-art methodologies suffer from the following three major limitations:

1) The HVAC control has not been considered together with the BMS for optimizing the driving range and/or battery lifetime.
2) They have all considered HVAC power consumption as a constant for modeling and estimation.
3) The effect of the HVAC power consumption on the battery lifetime has not been accounted.



DAC '15, June 07 - 11, 2015, San Francisco, CA, USA
Copyright 2015 ACM 978-1-4503-3520-1/15/06$15.00
http://dx.doi.org/10.1145/2744769.2744804

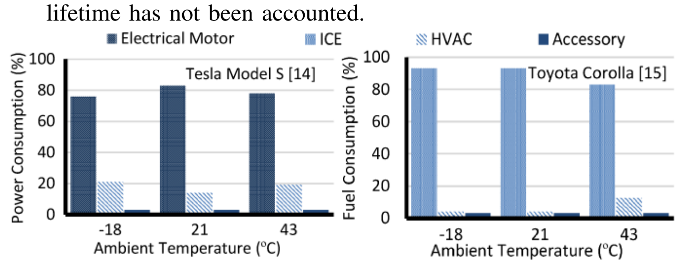


Fig. 1. Percentages of Three Types of Power Consumption in EV [14] and ICE Vehicle [15] for Different Ambient Temperatures.

### A. *Motivational Case Study on HVAC Load Analysis*

According to existing data, we have analyzed the power consumption in an EV (Tesla Motor S 60KWh [14]) and an Internal Combustion Engine (ICE) vehicle (Toyota Corolla [15]) when the HVAC is powered on, for different ambient temperatures (Fig. 1). Although the electrical motor efficiency in EVs and engine efficiency in ICE vehicles change for different ambient temperatures, their consumption is almost similar for different temperatures. Also, the accessories (e.g. entertainment system) in EVs and ICE vehicles consume the same small amount for different ambient temperatures. However, the HVAC consumption demonstrates different behavior for EVs and ICE vehicles. In lower temperatures, the HVAC in ICE vehicles uses the heat generated from the engine to warm up the cabin, resulting in almost no fuel consumption except for the fan. While, in higher temperatures, the HVAC has to consume power/fuel to cool down the air. On the other hand, in EVs, since almost no heat is generated from the electrical motor, the HVAC has to consume power in both cases to warm up or cool down the cabin. Moreover the percentage, the HVAC contributes to the total power consumption in EVs (upto 20%), is more significant than in ICE vehicles (upto 9%).

Therefore, this may affect the battery lifetime and EV driving range significantly, and due to the longer recharging time and relatively less number of charging stations, it may further worsen the situation for the driver and causes range anxiety [7].

**Summary and conclusion from observations:** the above analysis illustrates that HVAC power consumption is a significant factor in EVs and varies based on the ambient temperature. Hence, not considering the HVAC and BMS while optimizing the battery lifetime and driving range, may not give the optimal solution. Having a detailed HVAC model which describes its behavior and characteristics in various states and with respect to different inputs, may help us to estimate the HVAC power consumption in the EV and analyze its effect on the battery lifetime [16]. In this way, we may control the HVAC and its power consumption in an optimum way to improve the driving range and reduce the SoH degradation. Hence, our novel automotive climate control methodology optimizes the driving range and battery lifetime using the co-ordination between the HVAC and BMS.

### B. Problem and Research Challenges

The problem of improving the battery lifetime and driving range poses the following key challenges:

1) Having an accurate modeling and estimation for HVAC's dynamics, power consumption, and influence on the battery lifetime.
2) Co-ordination between the HVAC and the BMS for optimizing the battery lifetime and driving range.

### C. Our Novel Contributions and Concept Overview

To address the above-mentioned challenges, a novel automotive climate control methodology for optimizing battery lifetime and driving range is proposed that employs:

1) **Modeling and Estimation of HVAC (Section II-C)** which describes the instantaneous power consumption and thermodynamic behavior of a HVAC in different states and conditions.
2) **Modeling and Estimation of Battery Lifetime (Section II-D)** that measures the battery SoH degradation by predicting the EV power consumption during a driving period which can be done by integrating the HVAC, power train, and battery lifetime degradation models into an EV model.
3) **Optimized Battery Lifetime-aware Automotive Climate Control (Section III)** that reduces the HVAC power consumption when the electrical motor is estimated to consume more. On the other hand, when the electrical motor power consumption is estimated to be low, there is enough slack for the HVAC to adjust the cabin temperature again or precool/preheat the cabin before the next peak in power consumption arrives. Therefore, the SoC deviation and the SoC average in a discharging/charging cycle will decrease and thereby improve the driving range and the battery lifetime. This controlling methodology is formulated using Model Predictive Control (MPC). Fig. 2 describes our novel battery lifetime-aware automotive climate control methodology.

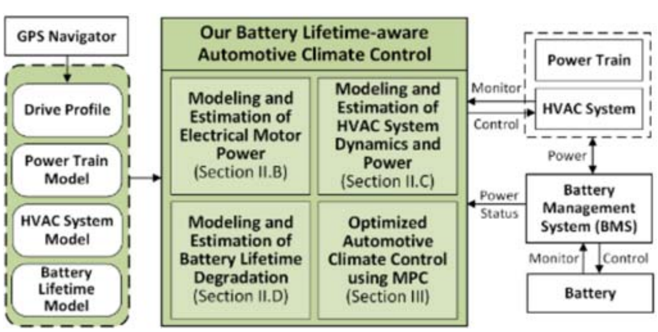


Fig. 2. Battery Lifetime-aware Automotive Climate Control Methodology.

## II. System Modeling and Estimation

As we have stated in Section I, the overall power consumption in EVs is categorized into three types; the electrical motor, HVAC, and accessories. The power train inside the EV, in which the electrical motor is the main component, contributes to driving. Hence, the electrical motor power consumption is mainly influenced by the vehicle speed, acceleration, and road slope (see Section II-B). The HVAC is another significant flexible power consumer inside the EV. The outside climate, e.g. the ambient temperature and solar radiation, influence the HVAC power consumption significantly (see Section II-C). However, the accessories power consumption is fixed and small compared to other two types.

Characteristics of the components inside an EV are modeled using Ordinary Differential Equations (ODE) to estimate their behavior and power consumption in different time instances. Also, the time-varying factors influencing the consumption, e.g. vehicle speed, acceleration, road slope, and ambient temperature, are modeled as a multi-variable input to the above-mentioned models (see Section II-A).

### A. Drive Profile

The total EV power consumption is mainly influenced by the surrounding environment. For instance, the HVAC power consumption is influenced by the ambient temperature and the electrical motor power consumption is affected by the vehicle speed, acceleration, and road slope. We define the term *drive profile* to model these time-varying factors as a multi-variable input data. A drive profile is a discrete-time sampled data from the environment, the EV is driving in. Nowadays, most drivers use GPS navigation systems to select the most appropriate route to their destinations. Hence, the route information and the parameters of each route segment such as: road slope, average vehicle speed, and average vehicle acceleration, are known accurately before driving. Also, there are existing databases that provide the information needed for generating real-life drive profiles. [17] provides the traffic flow information and the average vehicle speed in each route segment. The elevation at different coordination in the route is measured to calculate the road slopes [17]. The ambient temperature at each route segment is extracted from the existing climate databases [18]. On the other hand, there exists standard driving cycles, e.g. NEDC, EUDC, etc. [3]. These driving cycles are mainly used for simulation, verification, and comparison of the EV efficiency, driving range, and battery lifetime.

### B. Power Train Model

The power train in EV is responsible for generating the required power using the electrical motor and transferring it to the wheels (see Fig. 3 for an example of a power train in EV, modeled by AMESim [19]).

In an EV, the main propulsion force - the tractive force ($F_{tr}$) - is provided by the electrical motor to overcome the road load force ($F_{rd}$) to propel the vehicle forward at a desired speed and acceleration [20]. $F_{rd}$ consists of the aerodynamic drag, the gravitational force, and the rolling resistance:

$$F_{rd} = F_{gr} + F_{aero} + F_{roll} \tag{1}$$

The aerodynamic drag ($F_{aero}$) is the viscous resistance of the air working against the vehicle motion which is quadratically proportional to the vehicle speed ($v$). The force is calculated as:

$$F_{aero} = \frac{1}{2}\rho_{air} C_x A \left(v + v_{wind}\right)^2 \tag{2}$$

where $\rho_{air}$ is the air density, $C_x$ is the aerodynamic drag coefficient, $A$ is the effective frontal area of the vehicle, and $v_{wind}$ is the head-wind velocity.

The gravitational force ($F_{gr}$) is the force caused by the gravity and is mainly dependent on the road slope. The force is calculated as:

$$F_{gr} = mg \sin\left(\arctan\left(\frac{\alpha}{100}\right)\right) \tag{3}$$

where $m$ is the total mass of the vehicle, $g$ is the gravitational acceleration constant, and $\alpha$ is the percentage of the road slope; 100% represents the slope of 45°.

The rolling resistance ($F_{roll}$) is produced by the flattening of the tire at the contact surface of the road and it is calculated as:

$$F_{roll} = mg\left(c_0 + c_1 v^2\right) \tag{4}$$

where $c_0$ and $c_1$ are the rolling resistance coefficients.

$F_{tr}$ is generated by the electrical motor to overcome $F_{rd}$ so that the vehicle maintains the desired acceleration ($a$) and speed:

$$F_{tr} = F_{rd} + ma \tag{5}$$

The electrical motor power consumption ($P_e$) is calculated as:

$$P_e = \frac{F_{tr} v}{\eta_m} \tag{6}$$

where $\eta_m$ represents the electrical motor efficiency when converting electrical to mechanical energy in the motor mode and converting mechanical to electrical energy in the generator mode (regenerative break). $\eta_m$ is highly dependent on the motor rotational speed and the generated torque.

The model parameters are adjusted based on the specifications of Nissan Leaf [12]. Its driving range and power consumption have been verified in different conditions by our model.

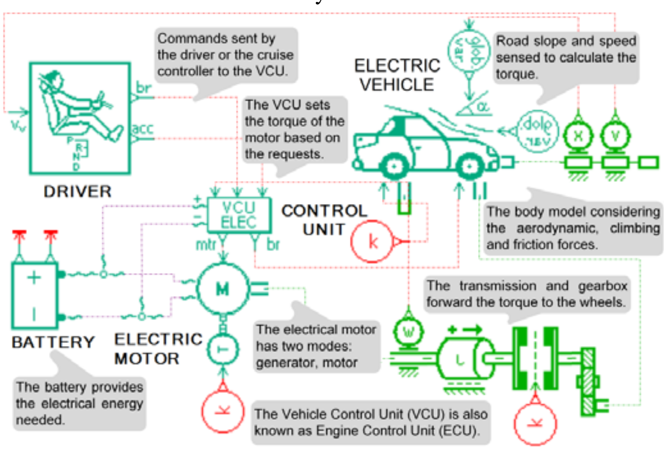


Fig. 3. Diagram of a Power Train in an EV Modeled by AMESim [19].

### C. HVAC Model

The HVAC in modern vehicles mainly uses the Variable Air Volume (VAV) system [10]. The advantage of this system is the precise control of the temperature and humidity in multi-zone or single-zone with lower energy consumption [10]. The HVAC structure [8][9] in an EV is depicted in Fig. 4. The system contains a variable-speed fan to provide the supply air to the zone(s). A valve damper is used to control the mix of the outside air and the recirculated air back into the system. The cooler and the heater will control the air temperature by exchanging heat. In this paper, we assume a single-zone HVAC and model the corresponding behavior and dynamics in different parts of the system using low-order ODEs. Despite the simplicity (compared to higher-order thermodynamic equations), the model provides sufficient information for analyzing the transient behavior of the system. The humidity can be an important factor affecting the HVAC power consumption, but it is not typically directly measured or controlled [21]. Therefore, in this paper, the temperature represents an equivalent dry air temperature at which the dry air has the same specific enthalpy as the actual moist air mixture.

The temperature inside the cabin (zone) ($T_z$) is influenced by the supply air to the cabin, the heat exchange with outside, and the solar radiation. The energy balance in the cabin model is described as:

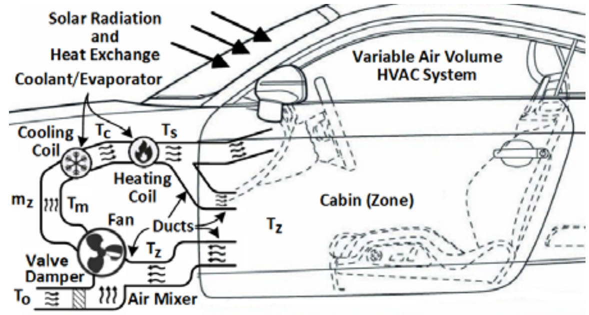


Fig. 4. The Structure of a Single-zone HVAC in an EV.

$$M_c \frac{dT_z}{dt} = \dot{Q} + \dot{m}_z c_p (T_s - T_z) \tag{7}$$

where $M_c$ is the thermal capacitance of the air, wall, and the seats inside the cabin and $c_p$ is the heat capacity of the air. The cabin temperature changing rate ($\frac{dT_z}{dt}$) is also controlled by the air flow rate into the cabin ($\dot{m}_z$).

The exchanged heat with outside and the solar radiation are modeled as thermal loads $\dot{Q}$:

$$\dot{Q} = \dot{Q}_{solar} + c_x A_x (T_o - T_z) \tag{8}$$

where the solar radiation ($\dot{Q}_{solar}$) and outside temperature ($T_o$) are time-varying factors. The value of $T_o$ is provided by the drive profile and $\dot{Q}_{solar}$ is assumed to be constant during driving (thermal load offset). The heat exchange through the walls with outside is proportional to the difference between $T_z$ and $T_o$, the heat exchange coefficient $c_x$, and the area separating the cabin and outside ($A_x$).

The air returned from the cabin is mixed with the outside air and recirculated back to the system. The fraction of the returned air from the cabin is $d_r$, which is controlled by a damper. Then, the energy balance in the air mixer gives the temperature of the system inlet air ($T_m$) as follows:

$$T_m = (1 - d_r) T_o + d_r T_z \tag{9}$$

where $T_z$ is the returned air temperature which is as same as the cabin temperature in a single-zone HVAC.

We consider the cooling and heating coil power consumption in terms of the energy difference between their inlet and outlet air flow. Moreover, the heat exchange between the coolant/evaporator and air is modeled as efficiency parameters:

$$P_h = \frac{c_p}{\eta_h} \dot{m}_z (T_s - T_c) \tag{10}$$

$$P_c = \frac{c_p}{\eta_c} \dot{m}_z (T_m - T_c) \tag{11}$$

where $P_c$ and $P_h$ are cooling coil and heating coil power consumption, respectively. $\eta_h$ and $\eta_c$ are the efficiency parameters describing the operating characteristics of the heating and cooling processes. The fan power consumption ($P_f$) is quadratically related to $\dot{m}_z$:

$$P_f = k_f (\dot{m}_z)^2 \tag{12}$$

where $k_f$ is a parameter that captures the fan efficiency and the duct pressure losses.

The parameters for the model have been set based on an HVAC specifications [8][9] and to match the thermodynamic behavior in different conditions accurately [15][22].

### D. Battery Lifetime Model

Lithium-ion batteries which are widely used as the primary electrical energy storage [23], demonstrate less usable capacity in higher discharge rates (rate-capacity effect). This characteristic is described using the Peukert's Law [3] and battery $SoC$ is calculated as:

$$SoC^t = SoC^0 - 100 \times \int_0^t \frac{I_{eff}}{C_n}\, dt \tag{13}$$

$$I_{eff} = I\left(\frac{I}{I_n}\right)^{pc-1} \quad (14)$$

where $C_n$ is the nominal capacity of the battery measured at the nominal current ($I_n$) predefined by the battery manufacturer. $I_{eff}$ represents the effective current draining the chemical energy. $pc$ is the Peukert's constant which is typically measured empirically for each type of battery cell. $SoC^t$ represents the SoC at time $t$.

Moreover, SoH - the ratio of the current capacity to the nominal capacity - degrades over time in Lithium-ion battery cells (capacity fade effect). The SoH degradation ($\bigtriangledown SoH$) is mainly influenced by the stress on the battery cell which may be modeled as SoC deviation ($SoC_{dev}$) and the SoC average ($SoC_{avg}$) [6]. $\bigtriangledown SoH$ is measured based on the SoC pattern over a time period:

$$\begin{aligned}\bigtriangledown SoH &= f\ (SoC_{dev}, SoC_{avg})\\ &= (a_1 e^{\alpha SoC_{\mathsf{dev}}} + a_2)(a_3 e^{\beta SoC_{\mathsf{avg}}}) \quad (15)\end{aligned}$$

where $\alpha$, $\beta$, $a_1$, $a_2$, and $a_3$ are the parameters for estimating $\bigtriangledown SoH$ accurately based on the battery type. Consideration of the battery temperature for estimating $\bigtriangledown SoH$ is out of the scope of the paper and is modeled as a constant in Eq. 15. $SoC_{dev}$ and $SoC_{avg}$ are calculated based on a discharging/charging cycle as:

$$SoC_{dev}^2 = \frac{1}{T}\int_0^T (SoC(t) - SoC_{avg})^2 dt \quad (16)$$

$$SoC_{avg} = \frac{1}{T}\int_0^T SoC(t)dt \quad (17)$$

where $T$ is the period of the discharging/charging cycle. However, in this paper, the charging part of the cycle is assumed to have fixed pattern and duration and the effect of it on $SoC_{dev}$ and $SoC_{avg}$ are modeled as constants. The battery cell capacity decreases with the rate of $\bigtriangledown SoH$. When the battery capacity reaches the 80% of its nominal capacity, it will be useless [6]. Therefore the number of discharging/charging cycles, the battery can be used (the battery lifetime), is dependent on $\bigtriangledown SoH$.

## III. Automotive Climate Control

The HVAC has multiple state variables that define the current condition of the system. Control inputs are adjusted by the automotive climate control to maintain the system output and state variables in a specific range and target. The evaluation of $\bigtriangledown SoH$ requires estimating the power consumption of the electrical motor and the HVAC. The estimation is done by inputting the drive profile (see Section II-A) into the models of the components (see Section II). A Model Predictive Control (MPC) [24] may be used for controlling the input variables of the HVAC. The MPC enables us to look into a receding horizon (control window) of the discharging cycle (driving cycle) and decide on the state variables and control inputs for minimizing the cost function, e.g. minimizing $\bigtriangledown SoH$. The larger the control window, the more variables there are to optimize and much more flexibility for considering the EV (physical plant) variations. In each time step, the MPC optimizes the state and input variables involved in the control window and tries to minimize the cost function which is also based on the state and output variables. The system model equations are nonlinear and non-convex, therefore the best option might be to apply Sequential Quadratic Programming (SQP) [21] as the optimization algorithm for the MPC in each time step.

### A. Optimal Control Formulation

Since the control is done in discrete-time, the model equations also need to be defined in discrete-time. For instance, Eq. 7 and 8 that model the cabin dynamics and solar radiation, are discretized as:

$$M_c\frac{T_z^+ - T_z}{\triangle t} = \dot{Q} + \dot{m}_z c_p(T_s - \frac{T_z^+ + T_z}{2}) \quad (18)$$

$$\dot{Q} = \dot{Q}_{solar} + c_x A_x(T_o - \frac{T_z^+ + T_z}{2}) \quad (19)$$

where $T_z^+$ represents the corresponding value at the next time step $t + \triangle t$. Here, $\triangle t$ is a time step duration (sample period).

The input variables to the power train model are $v$, $\alpha$, and $a$ (see Section II-B). Let $d^t = [v, \alpha, a]^0$ be the value of the input vector to the power train model at time $t$ and ${P_e}^t$ be the estimated value of the electrical motor power consumption.

In the HVAC, let $x^{k|t}$ be the value of the state variable $T_z$, $i^{k|t}$ be the value of the controlling input vector $[T_s, T_c, d_r, \dot{m}_z]^0$, and $u^{k|t}$ be the vector of auxiliary variables $[T_m, P_h, P_c, P_f, P_e, SoC]^0$ at time $t + k \triangle t$, predicted at time $t$.

The control requirements and restrictions state the following time-varying constraints on control inputs and state variables:

*C1:* $\underline{\dot{m}}_z \le \dot{m}_z \le \overline{\dot{m}}_z$ maximum and minimum air flow to the cabin
*C2:* $\underline{T_z} \le T_z \le \overline{T_z}$ comfort zone restrictions on cabin temperature
*C3:* $T_c \le T_s$ heater always increases the temperature
*C4:* $T_c \le T_m$ cooler always decreases the temperature
*C5:* $\underline{T}_c \le T_c$ minimum outlet air temperature by cooler
*C6:* $T_s \le \overline{T}_h$ maximum outlet air temperature by heater
*C7:* $0 \le d_r \le \overline{d}_r$ limitation on recirculated air fraction
*C8:* $P_h \le \overline{P}_h$ heater maximum power output
*C9:* $P_c \le \overline{P}_c$ cooler maximum power output
*C10:* $P_m \le \overline{P}_m$ fan maximum power output

also, inside the control window, the predicted value for $T_z^+$ at time $t + k \triangle t$ should be equal to $T_z$ at the next predicted time step $t+(k+1)\triangle t$. The initial condition for $T_z$ is described by $x_{0|t} = T_z^t$.

The model equations, system dynamics, and constraints can all be expressed in the following form:

$$F_j\left(\begin{bmatrix} x^{k|t} \\ i^{k|t} \\ u^{k|t} \\ x^{k+1|t}\end{bmatrix}\right) = 0 \qquad A^{k|t}\begin{bmatrix} x^{k|t} \\ i^{k|t} \\ u^{k|t} \\ x^{k+1|t}\end{bmatrix} \le b^{k|t} \quad (20)$$

where $F_j$ is the $j^{th}$ non-linear equality constraint function for the optimization problem. The matrices $A^{k|t}$ and $b^{k|t}$ define the linear inequality constraints at time $t + k \triangle t$.

The discretized cost function for the optimization problem is modeled through the following quadratic equation:

$$\begin{aligned}C = \sum_{\tau=t}^{t+N\triangle t} & w_1(P_f + P_c + P_h) + w_2(SoC - SoC_{avg})^2\\ & + w_3(T_z - T_{target})^2 \quad (21)\end{aligned}$$

where $N$ is the number of time steps in the control window of the MPC, $w_1(P_f + P_c + P_h)$ is for optimizing the HVAC power consumption with the weight value of $w_1$, $w_2(SoC - SoC_{avg})$ optimizes $\bigtriangledown SoH$ by minimizing $SoC_{dev}$ with the weight value of $w_2$, and $w_3(T_z - T_{target})^2$ stabilizes the cabin temperature around the target temperature ($T_{target}$) with the weight value of $w_3$. It needs to be mentioned that the direct equation of $\bigtriangledown SoH$ is not used in the cost function, since its non-linearity caused the optimizer not to converge most of the time.

### B. MPC Control Algorithm

The algorithm in our automotive climate control methodology calculates the electrical motor power consumption using the input drive profile, and solves the optimization problem based on Eq. 20 and 21 at each time step, to find the optimum input control values.

Algorithm 1 illustrates a pseudo-code to simulate the driving-time controlling process of a HVAC inside an EV considering the battery lifetime for a given drive profile D.

**Algorithm 1:** Battery Lifetime-aware Automotive Climate Control

```
   Input: Drive profile D
   Output: Estimated 5 SoH
1  T = length (D)
   // extract route information for power train
2  d   D[v; a; □]
3  for t = 1 to T do
4  │  e^t = PowerTrain (d^t)
5  │  // measure electrical motor power consumption
6  N = control window duration
7  x = N □ 1 matrix                          // state variable
8  i = N □ 4 matrix                          // control inputs
9  u = N □ 6 matrix                      // auxiliary variables
10 x^+ = N □ 1 matrix                        // state variable
11 x^0   T_init                // initial cabin temperature
   // control window optimization variables
12 z   [x; i; u; x^+]^0
   // driving-time HVAC controlling starts
13 for t = 1 to T do
14 │  P_e    f e^k jt □ k □ t + N g
15 │  T_o    f D [T_o]^k jt □ k □ t + N g
16 │  z_opt = Optimize (z)                     // call optimizer
17 │  // apply control inputs & measure the states
18 │  [T_z^+; P_f; P_c; P_h] = HVAC (z_opt)
19 │  P^t    P_e + P_f + P_c + P_h
20 │  SoC^+ = BMS (P^t)        // measure next SoC by BMS
21 │  x^0    T_z^+     // next time step cabin temperature
22 │  u^0[SoC]    SoC^+              // next time step SoC
23 return 5 SoH = Battery (P)
```

First, the route information is extracted from the drive profile (line 2) to measure the electrical motor power consumption, vector $e$ (lines 3-5). The number of the time steps in the control window for MPC is defined in line 6. The state variables ($x$, $x^+$), control inputs ($i$), and auxiliary variables ($u$) for the control window are defined (lines 7-10) and combined in a vector as optimization variables ($z$) (lines 12). The cabin temperature, the state variable ($x$) at the starting time, is initialized (line 11). In lines 13-22, the driving-time controlling of the HVAC is in progress. The electrical motor power consumption and the ambient temperature for the control window which have been estimated are stored in $P_e$ and $T_o$, respectively (lines 14-15). The optimizer is called to solve the optimization problem stated in Eq. 20 and 21 and returns the optimum solution (line 16). The optimum solution is applied to the HVAC (physical plant) and the new cabin temperature and HVAC power consumption are measured (line 18). The total EV power consumption is calculated and stored at index $t$ of the vector $P$ (line 19). The battery SoC is measured by the BMS using Eq. 13 (line 20). The cabin temperature and battery SoC at time $t$ is used as the initial condition for the next time instance $(t+1)$ (lines 21-22). Finally, $\bigtriangledown SoH$ for the drive profile is calculated by inputting the vector $P$ to the battery model described in Eq. 15 and returned (line 23).

## IV. Experimental Results

### A. Experimental Setup

The model equations defined in Section II contain multiple parameters which are mostly defined by the real-life specifications of the system. The values of the parameters are set and adjusted so that the system dynamics are verified by the experimental data gathered from the existing references. Our battery lifetime-aware automotive climate control in Section II and III is implemented in MATLAB/Simulink [25] and an EV is modeled using AMESim (commercial system-level automotive design tool) [19] as the physical plant of the MPC. For evaluation, we use multiple standard driving cycles as the drive profiles and conduct co-simulation using these two platforms.

### B. Comparison to State-of-the-Art

We compare our battery lifetime-aware automotive climate control methodology with *1) switching On/Off methodology [8][9] and 2) fuzzy-based methodology [10]*. As our methodology is dependent on the drive profile, for fairness of the comparisons, all methodologies have been applied for the same system model, drive profile, and comfort zone.

**1) Cabin Temperature Analysis:** in each methodology, the controller sets the variables in the HVAC for optimizing the cost function and reaching a target. As shown in Fig. 5, the controllers manage the cabin temperature during driving-time differently. For instance, as shown in Fig. 5, the cabin temperature fluctuates the maximum when using the switching On/Off methodology, while the fuzzy-based methodology stabilizes the temperature as far as possible.

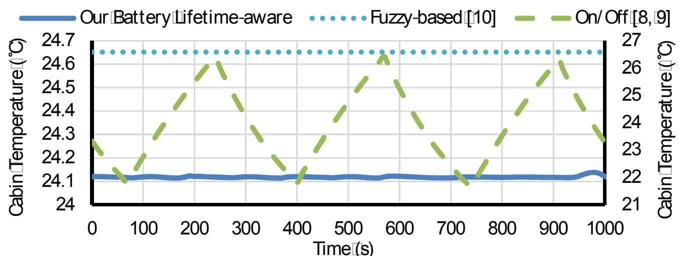


Fig. 5. Cabin Temperature Analysis for Different Controllers [right Y-axis is for On/Off methodology and left Y-axis is for our battery lifetime-aware and fuzzy-based methodologies].

On the other hand, as shown in Fig. 6, our methodology demonstrates different temperature management; it reduces the HVAC consumption when the electrical motor is consuming high power and it would precool the cabin (in this case outside is warmer) before the electrical motor consumption gets higher. In this way, the electrical motor consumption would be complemented by the HVAC consumption.

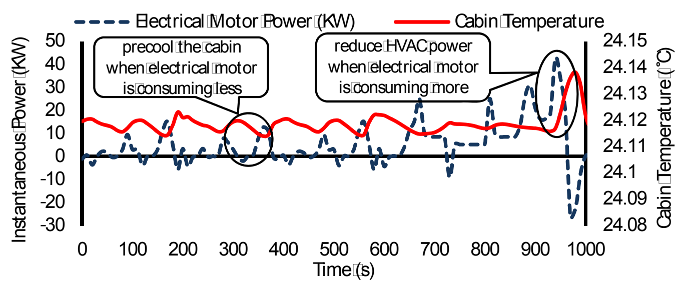


Fig. 6. Illustrating the Precool Process using Our Algorithm.

**2) Battery Lifetime Analysis:** SoH degradation may vary based on the methodologies. We have set the same ambient temperature, comfort zone, and target temperature for all the methodologies. Then, we have compared the $\bigtriangledown SoH$ and listed their ratios with respect to the first controller (switching On/Off) in Fig. 7. As shown in the figure, the $\bigtriangledown SoH$ has been improved the most in *ECE_EUDC* drive profile. The improvement (on average 14%) in our methodology is due to the controller that is trying to minimize the SoC deviation by adjusting the HVAC power consumption (as shown in Fig. 6).

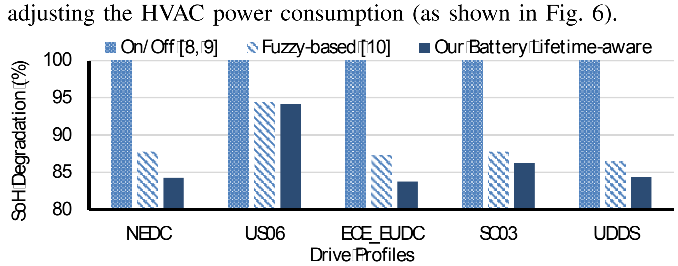


Fig. 7. Battery Lifetime Comparison for Different Drive Profiles.

**3) HVAC Power Consumption Analysis:** the average HVAC power consumption may vary by the methodology used and its variables. We have set the same ambient temperature, comfort zone, and target temperature for all the methodologies. Then, we have been able to compare the average HVAC power consumption and illustrate it in Fig. 8. As shown in the figure, our methodology minimizes the power consumption as far as possible (on average 39%). Although this improvement is marginal compared to the fuzzy-based methodology (on average 6%), our methodology has improved $\bigtriangledown SoH$ by minimizing the SoC deviation (see Fig. 7).

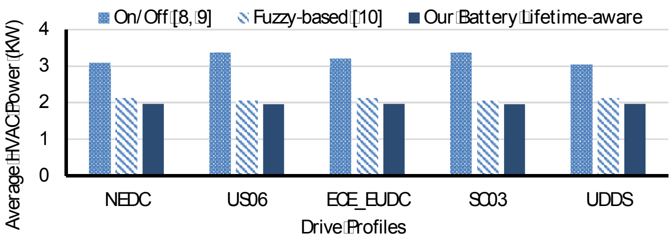


Fig. 8. HVAC Power Consumption Analysis for Different Drive Profiles.

**4) Ambient Temperature Analysis:** the controllers for different methodologies must maintain the cabin temperature in the comfort zone regardless of the outside temperature. However, they show different efficiency and $\bigtriangledown SoH$ in different conditions. We compare the $\bigtriangledown SoH$ and HVAC power consumption in different ambient temperatures. In this comparison, *ECE_EUDC* drive profile has been used and the results for the HVAC power consumption and $\bigtriangledown SoH$ improvement compared to the respective methodology, are listed in Table I. Results show that in the conditions when the HVAC power consumption is more considerable, our methodology demonstrates more improvement in $\bigtriangledown SoH$ (as high as 36%).

TABLE I. ANALYSIS OF HVAC POWER CONSUMPTION AND SOH DEGRADATION FOR DIFFERENT AMBIENT TEMPERATURES.

| Ambient Temperature | Average HVAC Power Consumption (KW) | | | SoH Degradation Improvement (%) | |
|---|---|---|---|---|---|
| | On/Off [8, 9] | Fuzzy-based [10] | Our Battery Lifetime-aware | On/Off [8, 9] | Fuzzy-based [10] |
| 43℃ | 5.44 | 3.51 | 3.59 | 19.57 | 1.18 |
| 35℃ | 3.20 | 2.11 | 1.97 | 16.24 | 6.08 |
| 32℃ | 2.12 | 1.59 | 1.40 | 14.92 | 7.54 |
| 21℃ | 0.90 | 0.58 | 0.29 | 12.33 | 9.36 |
| 10℃ | 4.71 | 1.85 | 1.68 | 32.83 | 4.89 |
| 0℃ | 6.08 | 5.12 | 2.84 | 31.82 | 36.48 |

## V. CONCLUSIONS

Based on our experiments, we have noticed that inside an EV, the HVAC consumes the most power after the electrical motor. However, its consumption is flexible and controllable by adjusting the HVAC variables. Therefore, we have presented a novel battery lifetime-aware automotive climate control methodology which is based on the coordination between the HVAC and BMS. The methodology employs a controller based on MPC to estimate and optimize the battery lifetime. The controller reduces the HVAC power consumption when the electrical motor is consuming significantly. When the electrical motor is consuming less or generating, the HVAC may consume more in order to maintain the temperature and precool/preheat the cabin. This methodology may reduce the stress on the battery and improve the battery lifetime and driving range. Our methodology demonstrates significant improvement in battery lifetime (on average 14%) and average power consumption (on average 39% reduction) compared to the state-of-the-art methodologies. The battery lifetime improvement may vary based on drive profiles and ambient temperature. In the conditions when the HVAC power consumption is more considerable, $\bigtriangledown SoH$ improvement is more significant (as high as 36%).

## REFERENCES


[1] M. Lukasiewycz and S. Steinhorst, “System Architecture and Software Design for Electric Vehicles,” *DAC’13 Proceedings of the Design Automation Conference*, pp. 1–6, 2013.

[2] United States Environmental Protection Agency ”Sources of Greenhouse Gas Emissions”. www.epa.gov., 2014.

[3] S. Park, Y. Kim, and N. Chang, “Hybrid Energy Storage Systems and Battery Management for Electric Vehicles,” *DAC’13 Proceedings of the Design Automation Conference*, pp. 1–6, 2013.

[4] S. Chakraborty, M. Lukasiewycz, C. Buckl, S. Fahmy, P. Leteinturier, and H. Adlkofer, “Embedded Systems and Software Challenges in Electric Vehicles,” *DATE’12 Proceedings of the Conference on Design, Automation & Test in Europe*, pp. 424–429, 2012.

[5] W. Chang, M. Lukasiewycz, S. Steinhorst, and S. Chakraborty, “Dimensioning and configuration of EES systems for electric vehicles with boundary-conditioned adaptive scalarization,” *Proceedings of the International Conference on Hardware/Software Codesign and System Synthesis (CODES+ISSS’13)*, pp. 1–10, 2013.

[6] A. Millner, “Modeling Lithium Ion Battery degradation in electric vehicles,” *IEEE Conference on Innovative Technologies for an Efficient and Reliable Electricity Supply*, pp. 349–356, 2010.

[7] K. Knoedler, J. Steinmann, S. Laversanne, S. Jones, A. Huss, E. Kural, D. Sanchez, O. Bringmann, and J. Zimmermann, “Optimal energy management and recovery for FEV,” *DATE’2012 Design, Automation & Test in Europe Conference*, pp. 683–684, 2012.

[8] K. Umezu and H. Noyama, “Air-Conditioning system For Electric vehicles (i-MiEV),” *SAE Automotive Alternate Refrigerant Systems Symposium*, 2010.

[9] R. Montgomery, “Fundamentals of HVAC control systems,” *Elsevier*, 2008.

[10] B. Ibrahim, M. Aziah, S. Ahmad, R. Akmeliawati, H. Nizam, A. Muthalif, S. Toha, and M. Hassan, “Fuzzy-based Temperature and Humidity Control for HVAC of Electric Vehicle,” *Procedia Engineering*, pp. 904–910, 2012.

[11] M. Lorenz, D. Fiala, M. Spinnler, and T. Sattelmayer, “A Coupled Numerical Model to Predict Heat Transfer and Passenger Thermal Comfort in Vehicle Cabins,” *SAE Technical Paper*, 2014.

[12] J. G. Hayes, R. P. R. de Oliveira, S. Vaughan, and M. G. Egan, “Simplified Electric Vehicle Power Train Models and Range Estimation,” *IEEE Vehicle Power and Propulsion Conference*, pp. 1–5, 2011.

[13] K. R. Kambly and T. H. Bradley, “Estimating the HVAC energy consumption of plug-in electric vehicles,” *Journal of Power Sources*, pp. 117–124, 2014.

[14] Tesla Motors Inc.”Tesla Model S Range”. www.teslamotors.com., 2014.

[15] L. Knibbs, R. D. Dear, and S. Atkinson, “Field study of air change and flow rate in six automobiles,” *Indoor air*, pp. 303–313, 2009.

[16] M. A. Al Faruque and F. Ahourai, “A Model-Based Design of Cyber-Physical Energy Systems,” *ASP-DAC’14 Proceedings of Asia and South Pacific Design Automation Conference*, pp. 97–104, 2014.

[17] Google Inc. ”Google API Web Services”. developers.google.com., 2014.

[18] National Oceanic and Atmospheric Administration ”National Climatic Data Center”. www.ncdc.noaa.gov., 2014.

[19] SIEMENS ”LMS Amesim”. www.siemens.com., 2014.

[20] K. Reif, “Fundamentals of Automotive and Engine Technology,” *Springer: Bosch professional automotive information*, 2014.

[21] A. Kelman and F. Borrelli, “Bilinear Model Predictive Control of a HVAC System Using Sequential Quadratic Programming,” *International Federation of Automatic Control World Congress*, pp. 9869–9874, 2011.

[22] K. D. Huang, S. C. Tzeng, T. M. Jeng, and W. D. Chiang, “Air-conditioning system of an intelligent vehicle-cabin,” *Applied Energy*, pp. 545–557, 2006.

[23] L. Lu, X. Han, J. Li, J. Hua, and M. Ouyang, “A review on the key issues for lithium-ion battery management in electric vehicles,” *Journal of Power Sources*, pp. 272–288, 2013.

[24] T. Wei, T. Kim, S. Park, Q. Zhu, S. X.-D. Tan, N. Chang, S. Ula, and M. Maasoumy, “Battery Management and Application for Energy-Efficient Buildings,” *DAC’14 Proceedings of the Design Automation Conference*, pp. 1–6, 2014.

[25] MathWorks ”MATLAB, Simulink”. www.mathworks.com., 2014.